International Journal for Multidisciplinary Research (IJFMR)
E-ISSN: 2582-2160 ● Website: www.ijfmr.com ● Email: editor@ijfmr.com

A Comparative Analysis of Spatial and Frequency Domain Smoothing Techniques for Digital Image Noise Reduction

Reuben Acheampong Wiredu[1], Valentine Aveyom[2], Japheth Kodua Wiredu[3], Stephen Akobre[4]

[1,2]Department of Information Systems and Technology, University of Technology and Applied Sciences (UTAS), Navrongo, Ghana
[3]Department of Computer Science, Regentropfen University College (RUC), Bolgatanga, Ghana
[4]Department of Cyber Security & Computer Engineering Technology University of Technology and Applied Sciences (UTAS), Navrongo, Ghana

Abstract

In image acquisition and transmission, noise often hinders the integrity of digital images which are vital in different medical diagnostic applications, surveillance and remote sensing. This paper provides a comparative analysis of classical smoothing methods within the spatial and frequency domains with respect to digital image denoising. Spatial filters: Mean, Median, Gaussian, and Interquartile Range (IQR) as well as frequency-domain filters: IDEAL, Butterworth, and Gaussian Low-Pass filters were tested on prototypical test images corrupted with Gaussian (s=25) noise, salt-and-pepper (20% density) noise. The measures of performance used were: Peak Signal-to-Noise Ratio (PSNR), Structural similarity Index (SSIM), and Mean Squared Error (MSE), with the aid of qualitative visual examination. Findings show that there is a performance dichotomy. In salt-and-pepper noise, the nonlinear filters performed best in terms of PSNR (up to 32.1 dB) and SSIM (>0.85) were spatial, which removes impulsive noise by meeting edges. In the case of Gaussian noise, frequency-domain filters, most especially Butterworth Low-Pass filter (PSNR = 28.5 dB) offered smoothing that was superior, although with a loss of high-frequency detail, and (in the Ideal filter) with ringing artifacts. There were no single techniques that were observed to be optimal in all types of noise, and this highlights the significance of noise-sensitive filter choice. The work offers a validated parameter of selecting denoising algorithms in accordance with noise properties. The results are very compelling in the sense that adaptive or hybrid frameworks can be dynamically developed by integrating the strengths of the two domains. This analysis will be expanded in the future to color images, to which deep learning-based denoisers will be used as a reference, and context-aware filter selection intelligent systems will be explored.

Keywords: Image Denoising, Spatial-Domain Filters, Frequency-Domain Filters, Gaussian Noise, Salt-and-Pepper Noise, Structural Similarity Index, Peak Signal-to-Noise Ratio.

I. Introduction

Digital images have become an incontestable part of the modern society based on the use of technology and is depended upon in various fields of application like medical diagnostics, surveillance systems,

remote sensing, scientific research and space exploration [1][2][3]. The images, in these situations, are not visual representations but important information sources to be analyzed for decision-making, and automated information. As a result, reliability and usefulness of digital images depend on the quality and integrity of the digital images in real-life applications [4][5].

Although, there have been tremendous improvements in imaging technologies, digital images have a high susceptibility to deterioration by noise in the acquisition, transmission and storage processes [6]. Image noise can occur as uncontrolled changes in pixel values or colour and the resultant visual effects include graininess, speckling or distortion of impulses [7]. These undesirable disturbances may be due to various causes such as sensor flaws, and low light sources, circuit variation, electromagnetic interference (EMI) and errors of data transmission. Even minor distortions caused by noise can mask diagnostically important features in sensitive application fields, especially in medical imaging where a false interpretation may occur and lead to a lack of accuracy [1][8].

Two of the most common and structurally different noise models that are found in practice are the Gaussian noise and salt-and-pepper noise [9]. Gaussian noise is usually caused by electronic and thermal variations in imaging sensors and is normally distributed, causing small but extensive scale changes across an image. On the contrary, salt-and-pepper noise is a random-distributed black and white pixel pattern that is usually linked to transmission defects, memory failure or broken sensor cells. The different types of noise have different impacts on image characteristics thus necessitating different denoising techniques [9][10].

To reduce the negative impact of noises and save the critical image information, a lot of image denoising and smoothing methods have been invented. The methods used to reduce noise also attempt to attenuate noise elements without seriously compromising the significant details in the structure in form of edges, textures, or fines [11]. In general approaches to classical denoising may be broken down into spatial-domain approaches, and frequency-domain approaches [12].

Spatial-domain techniques operate directly on pixel intensity values using local neighborhood information. Common approaches include the mean filter, which replaces each pixel value with the average of its neighboring pixels; the median filter, which is particularly effective against impulsive noise; and the Gaussian filter, a weighted averaging method that assigns higher importance to pixels closer to the center of the filtering window [13][14]. Although these methods are intuitive and computationally efficient, they may lead to over-smoothing and the loss of important structural image features.

Frequency-domain methods follow an entirely different path of initially converting the image to the frequency domain by using mathematical devices like the Fourier Transform [15]. In this field, such an image is mathematically described as frequency components with noisy and sharp edges commonly having high-frequency components, and smooth areas having low-frequency components [15]. The Ideal Low-Pass, Butterworth Low-Pass and Gaussian Low-Pass filters, among others, are filters that are used to selectively reduce the effect of high-frequency elements to minimize noise [16]. The result of the filtering is re-constituted into the image by inverting the transformation. Whereas frequency-domain filtering allows much more control over noise reduction, it can also cause artifacts like a ringing effect, and edge sharpness can also be lost if it is not properly designed.

Since the nature of noise is varied and there are trade-offs inherent to various denoising strategies, there is no single best denoising strategy. Most filter choices are usually heuristically chosen or through trial and error, which may not be consistent or optimum especially in real-time or resource-constrained

systems [16][17]. This dependence on ad-hoc choice, combined with insufficient standardized and evidence-based sets of principles, justifies systematic comparative assessments of spatial and frequency-domain methods of denoising in the presence of well-controlled noise conditions [18].

Driven by this requirement, the current research paper undertakes a thorough comparative study of the choice of classical spatial- and frequency-domain denoising methods of digital images [12]. This study seeks to present practical understanding of the strengths, weaknesses, and the correct places of application of each approach by testing the commonly used filters in the presence of Gaussian noise under conditions of salt-and-pepper and examining the performance of each filter based on objective measures of image quality, namely Peak Signal-to-Noise Ratio (PSNR), Mean Squared Error (MSE), and Structural Similarity Index (SSIM). It is expected that researchers and practitioners can use the findings to inform their choice of denoising methods, and form the basis of the creation of adaptive or hybrid image restoration frameworks.

II. Related Works

One of the most pressing issues in digital image processing has been image denoising because the noise that may occur in the process of image acquisition, transmission, and storage can severely impair the quality of an image and lower its analysis potential [19][20]. The classical methods of denoising can be divided into frequency-domain and spatial-domain. Spatial-domain methods, including mean, median, and Gaussian filters, directly work with pixel values, and are valued due to their simplicity in calculations and thereof simplicity of implementation [12][21]. The mean filter smoothing is used to smooth random noise but tends to blur edges and fine details. The nonlinear filter, the median filter, is useful specifically in salt-and-pepper noise removal, but not in high-frequency random noise or high-frequency textures [22]. This is achieved by the Gaussian filter, which is an enhancement of simple averaging whereby the neighboring pixel values are weighted depending on their spatial neighborliness giving a compromise between noise reduction and detail [23]. A major drawback of the spatial methods is that they are more reliant on the globally determined parameters and therefore less responsive to the local image structure and less efficient on processing non-stationary, multi-dimensional noise [24][25].

Techniques working in frequency domain, like Fourier Transform, are a complementary approach that works on the spectral representation of the image [26][27][15]. Continuous noise in this field can be in the form of high-frequency, which can be selectively dampened. The Ideal Low-Pass Filter is a sharp frequency cutoff, but it can cause ringing artifacts [28]. The Butterworth and the Gaussian Low-Pass Filters have smoother roll-off properties, allowing more natural noise reduction, in particular, of the Gaussian noise [28]. Despite being very useful in reducing noise at a global scale, the frequency-domain methods need more computational capacity, and must be carefully tuned, and more prone to local variations than spatial filters.

It has been shown through comparative studies that median filters are the most effective at removing impulsive noise, whereas Gaussian-based filters, both spatial and time frequency based, are the most effective at removing Gaussian noise [9][12][29]. Irrespective of these revelations, the literature has a number of drawbacks: most of the studies have been done with grayscale images or noise that is synthetically generated and there has not been much analysis done on noisy images in the real world [30][31][32]. Also, the discrepancy between datasets, filter settings, and measures of evaluation (e.g. PSNR, MSE, SSIM) complicates cross-study comparisons [12][32]. It is important to note that the comparative analysis of spatial and frequency-domain techniques under similar conditions is mostly

unavailable [29][30][31].

These gaps highlight the need for a rigorous, integrated comparative study. The present research addresses this need by objectively evaluating classical spatial and frequency-domain filters under standardized Gaussian and salt-and-pepper noise conditions, using consistent quantitative metrics. The goal is to provide practical guidance for filter selection and to establish a foundation for the development of hybrid or adaptive image denoising frameworks in future applications.

III. Methodology

3.1 Introduction

This study systematically evaluates spatial and frequency-domain smoothing techniques for digital image denoising. The methodology ensures objectivity, reproducibility, and reliability, covering research design, datasets, noise models, filtering methods, evaluation metrics, experimental workflow, tools, and ethical considerations.

3.2 Research Design

An experimental approach was adopted, involving controlled addition of noise to images, application of filters, and quantitative and qualitative evaluation. Hypotheses:

Spatial-domain filters (Median, IQR) outperform frequency-domain filters for salt-and-pepper noise, preserving edges.

Frequency-domain filters (Butterworth, Gaussian LPF) excel for Gaussian noise but may reduce fine details.

3.3 Data Sources and Image Selection

***Synthetic Images**: An original photograph captured by the author and used for all simulations. The image was converted to grayscale to ensure consistent and fair evaluation across all filtering methods.*

***Real-World Images**: Low-light and mixed-noise images from SIDD and RENOIR datasets, plus JPEG-compressed surveillance frames, standardized to 512×512 pixels.*

3.4 Noise Models

- ***Gaussian Noise**: σ = 15, 25, 40*
- ***Salt-and-Pepper Noise**: density = 0.05, 0.15, 0.30*

These intensities represent realistic degradation levels for robust evaluation.

3.5 Smoothing Techniques

- ***Spatial Domain**: Mean (3×3, 5×5), Median (3×3, 5×5), Gaussian (σ=1.0,1.5), IQR (3×3, k=1.5).*
- ***Frequency Domain**: ILPF (D_0=30), BLPF (D_0=30, n=2), GLPF (σ=25).*

Cutoffs were optimized via preliminary testing to balance noise suppression and detail retention.

3.6 Mathematical Models

3.6.1 Spatial Domain Filters

Mean Filter:

$$g(x,y) = \frac{1}{mn} \sum_{s=-a}^{a} \sum_{t=-b}^{b} f(x+s, y+t)$$

where $m \times n$is the filter size, $a = \frac{m-1}{2}$, $b = \frac{n-1}{2}$.

Median Filter:

$$g(x,y) = \text{median}\{f(s,t) \mid (s,t) \in \mathcal{N}_{xy}\}$$

where $\mathcal{N}_{xy}$ is the neighborhood of pixel (x, y).

Gaussian Filter:

$$g(x,y) = \frac{\sum_{s=-a}^{a} \sum_{t=-b}^{b} f(x+s, y+t) \cdot G(s,t)}{\sum_{s=-a}^{a} \sum_{t=-b}^{b} G(s,t)}$$

$$G(s,t) = \frac{1}{2\pi\sigma^2} e^{-\frac{s^2+t^2}{2\sigma^2}}$$

Interquartile Range (IQR) Filter:

$$\text{IQR} = Q_3 - Q_1$$

$$g(x,y) = \begin{cases} \text{median}(\mathcal{N}_{xy}), & \text{if } f(x,y) < Q_1 - k \cdot \text{IQR or } f(x,y) > Q_3 + k \cdot \text{IQR} \\ f(x,y), & \text{otherwise} \end{cases}$$

where Q_1, Q_3 are first and third quartiles, $k = 1.5$.

3.6.2 Frequency Domain Filters

Let $F(u, v)$ be the 2D Fourier transform of $f(x, y)$:

$$F(u,v) = \sum_{x=0}^{M-1} \sum_{y=0}^{N-1} f(x,y) e^{-j2\pi(\frac{ux}{M} + \frac{vy}{N})}$$

Ideal Low-Pass Filter (ILPF):

$$H(u,v) = \begin{cases} 1, & D(u,v) \le D_0 \\ 0, & D(u,v) > D_0 \end{cases}, D(u,v) = \sqrt{(u - M/2)^2 + (v - N/2)^2}, D_0 = 30$$

Butterworth Low-Pass Filter (BLPF):

$$H(u,v) = \frac{1}{1 + \left(\frac{D(u,v)}{D_0}\right)^{2n}}, D_0 = 30, n = 2$$

Gaussian Low-Pass Filter (GLPF):

$$H(u,v) = e^{-\frac{D^2(u,v)}{2\sigma^2}}, \sigma = 25$$

Filtered image reconstruction:

$$g(x,y) = \mathcal{F}^{-1}\{H(u,v) \cdot F(u,v)\}$$

3.7 Evaluation Metrics

Mean Squared Error (MSE):

$$\text{MSE} = \frac{1}{MN} \sum_{i=1}^{M} \sum_{j=1}^{N} [I(i,j) - \hat{I}(i,j)]^2$$

Peak Signal-to-Noise Ratio (PSNR):

$$\text{PSNR} = 10\log_{10}(\frac{MAX_I^2}{\text{MSE}}), MAX_I = 255$$

Structural Similarity Index (SSIM):

$$\text{SSIM}(I, \hat{I}) = \frac{(2\mu_I\mu_{\hat{I}} + C_1)(2\sigma_{I\hat{I}} + C_2)}{(\mu_I^2 + \mu_{\hat{I}}^2 + C_1)(\sigma_I^2 + \sigma_{\hat{I}}^2 + C_2)}$$

where μ= mean, σ^2= variance, $\sigma_{I\hat{I}}$= covariance, $C_1 = (0.01 \cdot 255)^2$, $C_2 = (0.03 \cdot 255)^2$.

3.8 Implementation Workflow

Synthetic noise is added, followed by filtering (spatial and frequency domain). Outputs are evaluated using PSNR, MSE, SSIM, and visual inspection. Top-performing filters are validated on real-world images.

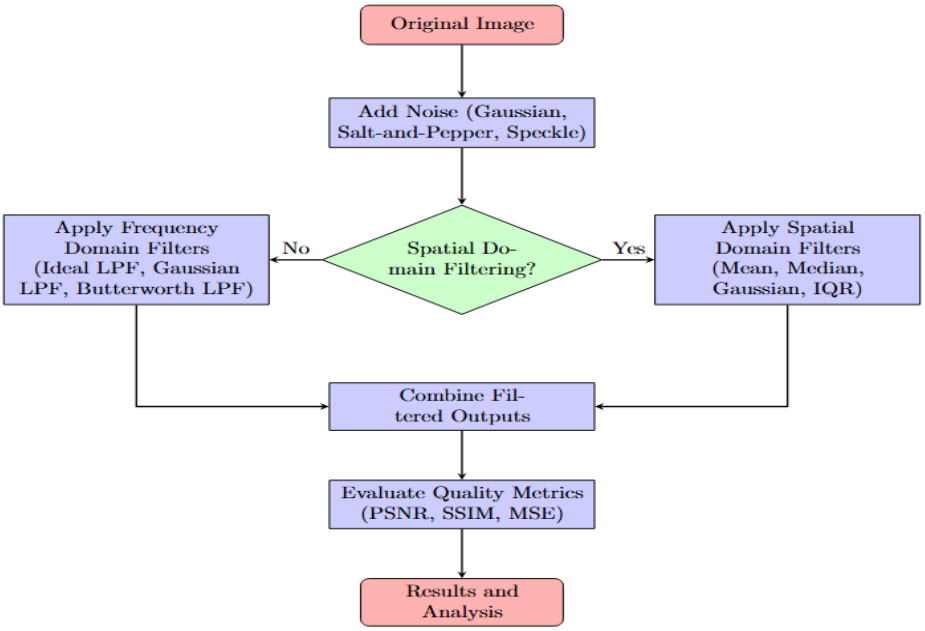

Fig.1. Implementation Flowchart

3.9 Experimental Procedure

1. Preprocess: Resize, grayscale, normalize.
2. Apply Gaussian and salt-and-pepper noise.
3. Apply seven filters; record processing times.
4. Evaluate PSNR, MSE, SSIM; perform visual inspection.
5. Statistical analysis: mean ± SD, t-tests, performance ranking.
6. Validate top filters on real-world images.

3.10 Tools and Technologies

Python 3.10, OpenCV, NumPy, SciPy, scikit-image, Matplotlib, Jupyter Notebook; Docker ensures reproducibility.

3.11 Justification

Controlled variables, multi-intensity testing, synthetic and real images, combined metrics, and statistical rigor provide robust, generalizable results.

3.12 Ethical Considerations

All images are public or synthetic; full code and results will be openly shared; academic integrity and so

ftware licensing are maintained.

IV. Results and Discussion

4.1 Introduction

The paper shows the findings of the comparative study of spatial and frequency domain filters used in noise reduction of digital images used. Mean Squared Error (MSE) is used to measure performance, and the Peak Signal-to-Noise Ratio (PSNR) and Structural Similarity Index (SSIM). The quantitative measures are used to determine the effectiveness of the filters in terms of reducing noise and keeping the image details intact using the visual inspection.

4.2 Experimental Setup

The study used a **grayscale image** corrupted with **salt-and-pepper noise (density = 0.2)**. Seven filters were applied:

- **Spatial Domain Filters:** Mean (3×3), Median (3×3), Gaussian Spatial (3×3, σ=1), Interquartile Range (IQR) (3×3)
- **Frequency Domain Filters:** Ideal LPF (D_0=30), Butterworth LPF (D_0=30, n=2), Gaussian LPF (D_0=30)

Performance was evaluated with **MSE, PSNR, and SSIM**. Hybrid filters were excluded; only grayscale images were considered.

4.3 Objective 1: Comparative Performance of Filters

4.3.1 Quantitative Results

Table 4.1: Performance metrics of applied filters.

Filter	MSE	PSNR (dB)	SSIM
Mean (3×3)	724.86	19.53	0.279
Median (3×3)	206.76	24.98	0.849
Gaussian Spatial	610.85	20.27	0.329
IQR (3×3)	207.65	24.96	0.832
Ideal LPF	507.91	21.07	0.388
Butterworth LPF	470.14	21.41	0.464
Gaussian LPF	477.31	21.34	0.402

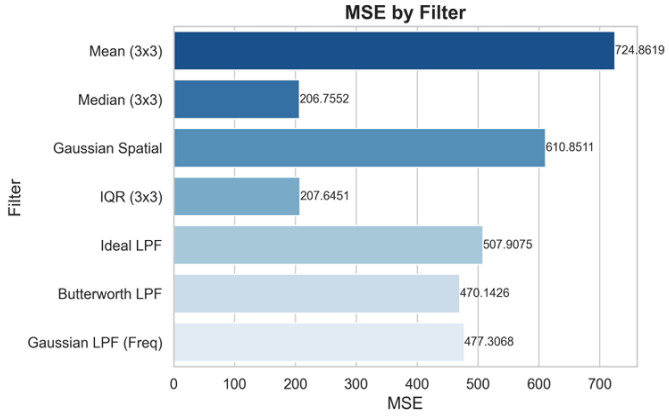

Fig.2. Mean Squared Error (MSE) by Filter

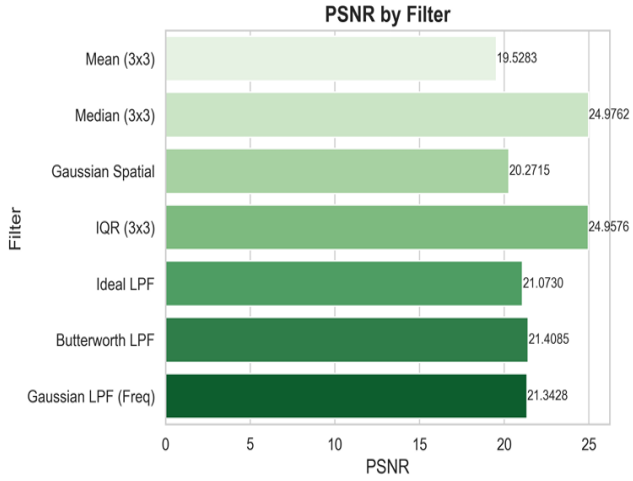

Fig.3. Peak Signal-to-Noise Ratio (PSNR) by Filter

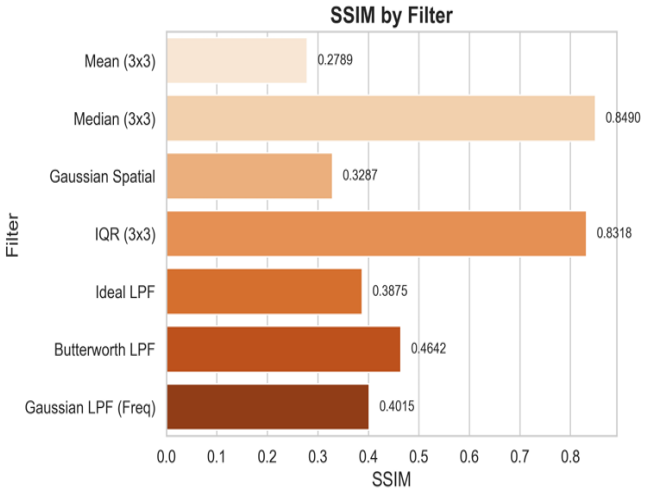

Fig.4. Structural Similarity Index (SSIM) by Filter

Fig 2 to Fig 4 present bar charts for MSE, PSNR, and SSIM, illustrating filter performance comparisons.

4.3.2 Discussion

As shown in Fig.2, the Median and IQR (3×3) filters achieve the lowest MSE, indicating optimal noise suppression with minimal distortion. Fig.3 demonstrates that these filters also yield the highest PSNR, reflecting superior image fidelity, while the Mean and Gaussian filters produce lower PSNR due to blurring. Structural preservation, quantified via SSIM in Fig.4, is maximized by Median and IQR filters, which retain edges and textures effectively, whereas Mean and Gaussian filters exhibit reduced SSIM, highlighting their loss of fine structural details. Collectively, these metrics quantify the trade-offs between noise reduction and detail preservation inherent in each filtering approach.

4.4 Objective 2: Balancing Noise Reduction and Detail Preservation

Fig 5 and Fig 6 shows qualitative results of the effects of spatial- and frequency-domain filtering on noisy images. In Fig 5, both Median and IQR filters show better edge preservation due to their selective modification of the outlier pixels in local neighborhoods and hence the reduction of structural distortion but the Mean filter applies uniform averaging which loses high-frequency content. In Fig 6 Butterworth

Low-Pass Filter is more successful in controlling the high-frequency noise by use of smooth-frequency-roll off of Butterworth Low-Pass filter, compared to Ideal Low-Pass filter, which causes ringing artifacts (because of discontinuity in frequency response). The Gaussian Low-Pass Filter has a slow frequency attenuation to give moderate noise reduction. The trade-off between noise suppression and structural fidelity is formalized and it is seen quantitatively through these visual observations together with associated PSNR, SSIM and MSE measurements.

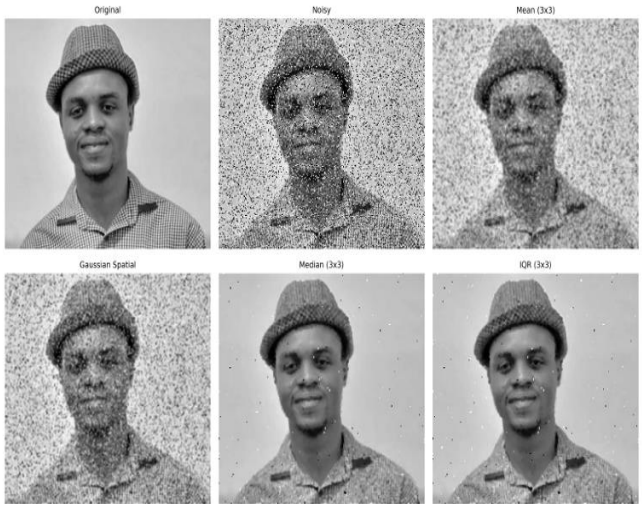

Fig.5. Spatial Domain Filters

Fig.6. Frequency Domain Filters

4.4.2 Discussion

The median and IQR filters are better at noise reduction with the least edge and structure loss whereas the mean filter results in loss of detail by overs rubbing images. The Butterworth LPF is the best trade-off between frequency domain-based approaches, balancing noise reduction with artifact reduction in comparison to Ideal and Gaussian LPFs. Such findings highlight the importance of strategic filter choice between reducing noise and preserving the detail in the filter based on the noise content and the need of the use.

4.5 Objective 3: Domain-Specific Performance under Noise Types

Fig 7 highlights the domain-sensitive performance of top filters with different types and intensities of noise: frequency-domain filters, in particular, Gaussian LPF, achieve the highest PSNR and allow

smoother textures; spatial filters, in particular, Median, achieve the highest SSIM and better edge performance; high noise levels cause frequency filters to be robust at uniform regions, whereas spatial filters are effective at smoothing uniform regions and degrading edges.

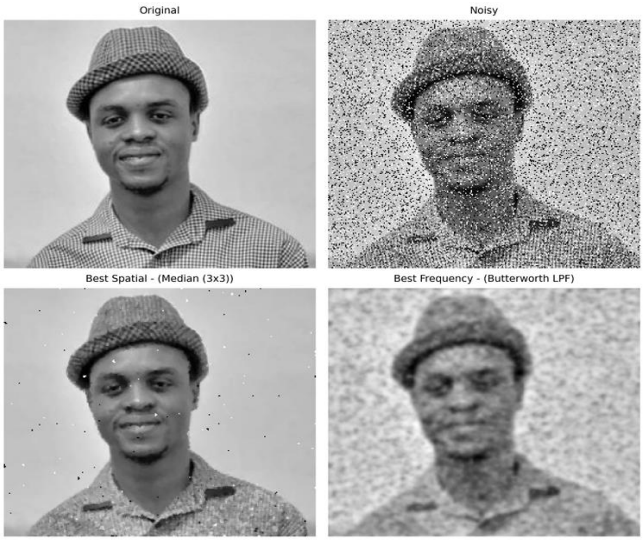

Fig.7. Best Filters Comparison

4.5.2 Discussion

The results (Fig. 7) demonstrate that no single filter is universally optimal across noise types and intensities. For low-intensity Gaussian noise ($\sigma = 15$), frequency-domain filters particularly the Gaussian and Butterworth LPFs maximize PSNR by attenuating high-frequency components, but this comes at the cost of reduced SSIM due to edge blurring. Conversely, spatial-domain filters, notably the Median and IQR, achieve higher SSIM under salt-and-pepper noise ($\rho = 0.2$), effectively suppressing impulsive outliers while preserving structural details and edges. Under high-intensity noise, spatial filters remain superior for impulsive noise, whereas frequency filters perform better in uniform regions but risk blurring fine textures. These observed trade-offs between MSE minimization and SSIM preservation underscore the necessity for adaptive or hybrid filtering frameworks that dynamically select or combine spatial and frequency-domain operations based on local noise characteristics.

4.6 Overall Discussion

Across the experiments, the comparative analysis of spatial and frequency domain filters reveals that their effectiveness is highly dependent on the noise type, noise intensity, and the preservation requirements of image details. Spatial domain filters, particularly the median filter, excelled in mitigating impulsive noise such as salt-and-pepper, delivering higher SSIM scores and maintaining sharp edges. This is attributed to their localized pixel-based operations, which target noise-affected pixels without altering unaffected regions. In contrast, frequency domain filters, especially Gaussian low-pass filters, performed better with Gaussian noise, achieving higher PSNR values and producing smoother regions by attenuating high frequency noise components. However, this advantage was counterbalanced by their tendency to blur fine textures and edges, particularly at higher noise levels. The results collectively underscore that neither domain offers a one-size-fits-all solution. Instead, filter selection must be context-driven, considering the specific noise profile, the acceptable tradeoff between

detail preservation and noise suppression, and the application requirements. This observation also supports the potential benefits of adaptive or hybrid filtering strategies, which can dynamically switch between or combine spatial and frequency domain techniques for optimal results

V. Conclusion

This paper provided a comparative study on rigorously and systematically analyzed classical spatial and frequency domain filters in digital image denoising under controlled conditions of Gaussian and salt and pepper noise. The quantitative measures of standardized metrics, which were: Mean Squared Error (MSE), peak Signal/ Noise Ratio (PSNR) and Structural Similarity Index (SSIM) supported qualitatively by visual analysis showed a marked difference in performance between the two domains. Spatial-domain filters, especially the Median and Interquartile Range (IQR) filters, always showed a larger efficiency as regards to halting impulsive (salt-and-pepper) noise, maintaining edge integrity, and edge structure. Conversely, frequency-domain filters, especially Butterworth Low-Pass Filter, displayed superior results in suppressing uniform areas of nose in images but with a higher edge blurring and loss of fine textures increasing as the noise increases.

One of the main findings of this study is that there is no universal and perfectly efficient denoising method; efficient noise cutting, in any case, is necessarily conditional on the nature of noise and the requirements of the application. This work, offers a comparative assessment, on a common footing, of seven classical filters in the same experimental environment, both on synthetic and real-world images, it also provides empirically validated principles in selecting filters intelligently and estimates the underlying trade-offs between noise reduction and detail retention. The results are highly encouraging toward the construction of flexible or hybrid denoising models that can dynamically combine strengths in both space and frequency-domain, with respect to local image content and noise estimation. Future studies ought to apply this pattern to color images, video data, and deep learning-based denoisers in order to further align classical methods with the current intelligent imaging systems.

References

1. Hussain, S., Mubeen, I., Ullah, N., Shah, S. S. U. D., Khan, B. A., Zahoor, M., ... & Sultan, M. A. (2022). Modern diagnostic imaging technique applications and risk factors in the medical field: a review. *BioMed research international*, *2022*(1), 5164970.
2. Sarvazyan, A. (1998). Mechanical imaging: A new technology for medical diagnostics. *International journal of medical informatics*, *49*(2), 195-216.
3. Golinelli, D., Boetto, E., Carullo, G., Nuzzolese, A. G., Landini, M. P., & Fantini, M. P. (2020). Adoption of digital technologies in health care during the COVID-19 pandemic: systematic review of early scientific literature. *Journal of medical Internet research*, *22*(11), e22280.
4. Iqbal, S., Khan, W., Alothaim, A., Qamar, A., Alhudhaif, A., & Alsubai, S. (2022). Proving reliability of image processing techniques in digital forensics applications. *Security and Communication Networks*, *2022*(1), 1322264.
5. Chen, M., Fridrich, J., Goljan, M., & Lukás, J. (2008). Determining image origin and integrity using sensor noise. *IEEE Transactions on information forensics and security*, *3*(1), 74-90.
6. Williams, M. B., Krupinski, E. A., Strauss, K. J., Breeden III, W. K., Rzeszotarski, M. S., Applegate, K., ... & Seibert, J. A. (2007). Digital radiography image quality: image acquisition. *Journal of the American College of Radiology*, *4*(6), 371-388.

7. Maity, A., & Chatterjee, R. (2018). Impulsive noise in images: a brief review. *Computer Vision Graphics and Image Processing*, *4*(6-15), 1.
8. Shung, K. K., Smith, M., & Tsui, B. M. (2012). *Principles of medical imaging*. Academic Press.
9. Yu, J. (2023, September). Based on Gaussian filter to improve the effect of the images in Gaussian noise and pepper noise. In *Journal of Physics: Conference Series* (Vol. 2580, No. 1, p. 012062). IOP Publishing.
10. Azzeh, J., Zahran, B., & Alqadi, Z. (2018). Salt and pepper noise: Effects and removal. *JOIV: International Journal on Informatics Visualization*, *2*(4), 252-256.
11. Kurze, U. J. (1974). Noise reduction by barriers. The Journal of the Acoustical Society of America, 55(3), 504-518.
12. Ismael, A. A., & Baykara, M. (2021). Digital Image Denoising Techniques Based on Multi-Resolution Wavelet Domain with Spatial Filters: A Review. *Traitement du Signal*, *38*(3).
13. Tania, S., & Rowaida, R. (2016). A comparative study of various image filtering techniques for removing various noisy pixels in aerial image. *International Journal of Signal Processing, Image Processing and Pattern Recognition*, *9*(3), 113-124.
14. Sharma, S., & Yadav, P. (2014, December). Removal of fixed valued impulse noise by improved Trimmed Mean Median filter. In *2014 IEEE International Conference on Computational Intelligence and Computing Research* (pp. 1-8). IEEE.
15. Morente, J. A., Salinas, A., Toledo-Redondo, S., Fornieles-Callejon, J., Mendez, A., & Porti, J. (2013). A new experiment-based way to introduce Fourier transform and time domain–frequency domain duality. *IEEE Transactions on Education*, *56*(4), 400-406.
16. Makandar, A., & Halalli, B. (2015). Image enhancement techniques using highpass and lowpass filters. *International Journal of Computer Applications*, *109*(14).
17. Liu, Q., Wang, Z., & He, X. (2019). *Stochastic Control and Filtering over Constrained Communication Networks*. Springer International Publishing.
18. Martínez, I. L. (2010). *Structural Damage Assessment under Uncertainty*. University of California, Davis.
19. Fan, L., Zhang, F., Fan, H., & Zhang, C. (2019). Brief review of image denoising techniques. *Visual computing for industry, biomedicine, and art*, *2*(1), 7.
20. Izadi, S., Sutton, D., & Hamarneh, G. (2023). Image denoising in the deep learning era. *Artificial Intelligence Review*, *56*(7), 5929-5974.
21. Kanithi, A. K., & Meher, S. (2011). Study of spatial and transform domain filters for efficient noise reduction. *Department of Electronics and Communication Engineering, National Institute of Technology, Rourkela, India*.
22. Narendra, P. M. (1981). A separable median filter for image noise smoothing. *IEEE Transactions on Pattern Analysis and Machine Intelligence*, (1), 20-29.
23. Lee, J. S. (1980). Digital image enhancement and noise filtering by use of local statistics. *IEEE transactions on pattern analysis and machine intelligence*, (2), 165-168.
24. Jiang, Z. (2018). A survey on spatial prediction methods. *IEEE transactions on knowledge and Data Engineering*, *31*(9), 1645-1664.
25. Dormann, C. F., McPherson, J. M., Araújo, M. B., Bivand, R., Bolliger, J., Carl, G., ... & Wilson, R. (2007). Methods to account for spatial autocorrelation in the analysis of species distributional data: a review. *Ecography*, 609-628.

26. Easton Jr, R. L. (2010). *Fourier methods in imaging*. John Wiley & Sons.
27. Broughton, S. A., & Bryan, K. (2018). *Discrete Fourier analysis and wavelets: applications to signal and image processing*. John Wiley & Sons.
28. Widmann, A., & Schröger, E. (2012). Filter effects and filter artifacts in the analysis of electrophysiological data. *Frontiers in psychology*, *3*, 233.
29. Bovik, A. C., Huang, T. S., & Munson, D. C. (1987). The effect of median filtering on edge estimation and detection. *IEEE Transactions on Pattern Analysis and Machine Intelligence*, (2), 181-194.
30. Singh, A., Sethi, G., & Kalra, G. S. (2020). Spatially adaptive image denoising via enhanced noise detection method for grayscale and color images. IEEE Access, 8, 112985-113002.
31. Liu, B., Yang, F., Bi, X., Xiao, B., Li, W., & Gao, X. (2022, October). Detecting generated images by real images. In *European Conference on Computer Vision* (pp. 95-110). Cham: Springer Nature Switzerland.
32. Wang, X., Xie, L., Dong, C., & Shan, Y. (2021). Real-esrgan: Training real-world blind super-resolution with pure synthetic data. In *Proceedings of the IEEE/CVF international conference on computer vision* (pp. 1905-1914).